Flow visualisation in a geotechnical centrifuge under controlled seepage conditions

Link:
[Link to publication record in Edinburgh Research Explorer](#)

Document Version:
Peer reviewed version

Published In:
Physical Modelling in Geotechnics

Flow visualisation in a geotechnical centrifuge under controlled seepage conditions

C.T.S. Beckett
School of Engineering, Institute for Infrastructure and Environment,
The University of Edinburgh, Edinburgh, Scotland, UK

A.B. Fourie
School of Civil, Environmental and Mining Engineering,
The University of Western Australia, Perth, WA

ABSTRACT: Image analysis is a powerful tool to obtain high-resolution displacement data from centrifuge models non-destructively. However, 'invisible' features, for example the phreatic surface, cannot be captured. Rather, analysis must rely on traditional measurement techniques, e.g. pressure transducers. Depending on the geotechnical complexity of the model, such discrete technologies might be insufficient. In this paper, we describe the processes used to inject a tracking fluid to visually identify flow patterns through a model slope. The merits of three tracing fluids were assessed: acrylic-resin ink ("artist's ink"); food-grade dye; and a fluorescent, low-viscosity dye (sodium fluorescein). Results showed that the developed injection technique was able to deliver the fluid without otherwise affecting seepage conditions. Depending on the fluid selected, the technique was equally able to examine the migration of a dense contaminant, assess model homogeneity or identify hidden flaws.

1 INTRODUCTION

Digital image analysis techniques are now commonplace when examining the behaviour of geotechnical centrifuge models (Stanier et al. 2015). The key advantage of such techniques is that high resolution data pertaining to the observed phenomenon can be obtained non-destructively. However, image analysis is clearly limited to visible phenomena: the position of the phreatic surface, for example, must be measured using more traditional, discrete measurement devices e.g. pressure transducers. For hydrostatic problems, such a system might be sufficient. However, such limited measurements might represent a considerable drawback when the flow conditions are unknown.

This work formed part of a larger study studying seepage characteristics of tailings storage facilities (TSFs): man-made geotechnical structures, often hundreds of metres high, formed by the progressive deposition of tailings slurry behind a retaining dam (Beckett et al. 2016, Beckett and Fourie 2016). Accurate control of the water balance in such systems is critical; of 22 TSF failures shortlisted by Blight and Fourie (2005), 7 could be said to be due to seepage-related phenomena, accounting for 268 deaths. The need to improve seepage characterisation in these structures is therefore obvious. In this paper, we discuss the development of a technique to visually track flow through a centrifuge model, under controlled seepage conditions, by injecting a tracing fluid; capturing the entire phreatic surface via image analysis would significantly improve confidence in groundwater level calculations and so those for TSF stability.

2 EXPERIMENTAL PROGRAMME

2.1 *Benchtop testing*

The fluid injection system discussed in this paper was designed to interface with centrifuge apparatus shown in Figure 1, described in Beckett et al. (2016). In that work, a syringe pump was used in a closed loop to control and monitor downstream seepage from a model embankment subjected to a hydraulic gradient. Here, we built on that apparatus to examine the ability of an additional syringe pump to inject a tracing fluid upstream of the model via the centrifuge's water supply. Critically, the developed system had to deliver the tracing fluid without affecting seepage conditions within the model: fluctuations in the delivered flow rate would result in lengthy re-equilibration times and, if significant, excessive centrifuge imbal-
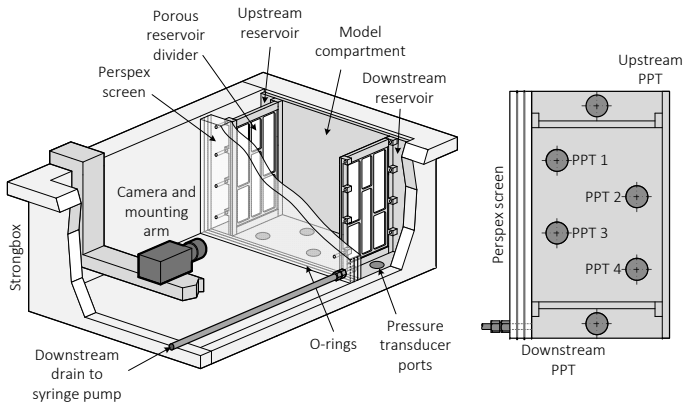
Figure 1: Centrifuge outer strongbox, model container and camera mounting (left) and pore pressure transducer (PPT) numbering (right). Note: downstream syringe pump not shown
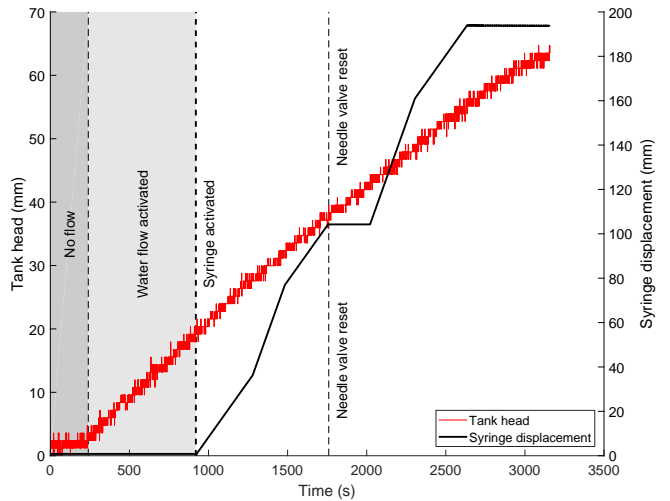

Figure 2: Injection system benchtop testing, showing key components

Figure 3: Change in tank head level with time during injection

Australia (UWA). Centrifuge models were housed within an outer $650\times390\times325$mm strongbox in a custom-designed container comprising two flanking reservoirs, a central model compartment and base-mounted pressure transducers (Figure 1). The container was equipped with a 25mm Perspex screen, fitted with photogrammetry tracking markers at 50mm vertical and horizontal intervals (photogrammetry was not used as part of the injection study but was used elsewhere). A small-format, five-megapixel resolution machine vision camera (Allied Vision Technologies Prosilica GC2450C) coupled with a Goya C-Mount 8mm focal length lens captured images of the models in-flight. Again, the centrifuge apparatus
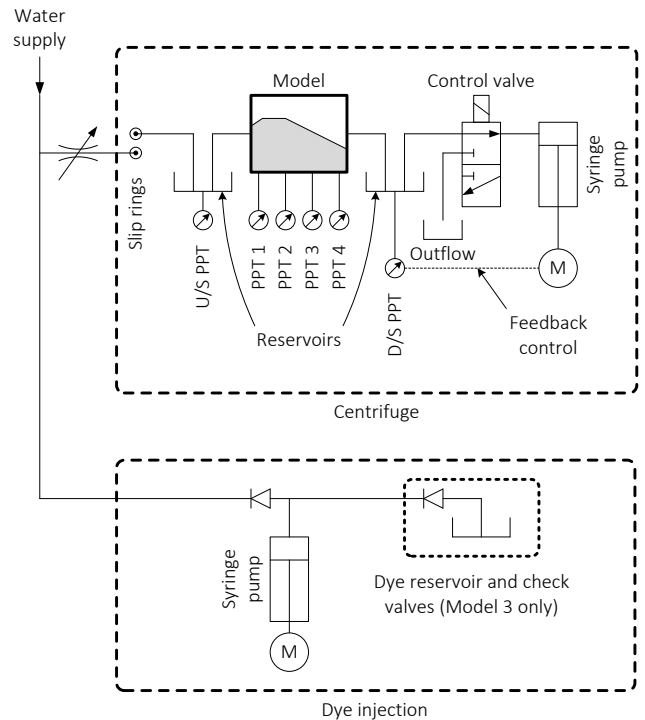
ance and potential safety concerns.

Benchtop testing was used to validate the proposed system under normal gravity (i.e. $1g$), shown in Figure 2. Water was fed into a measuring tank directly from the centrifuge water supply to ensure a realistic delivery pressure. Flow into the tank was controlled by a needle valve and measured via a pressure transducer mounted in the tank's base. Tracer fluid (here, acrylic-resin ink) was injected upstream of the needle valve (via a mixing loop) into the water supply at various rates; head levels in the tank during injection are shown in Figure 3. Head levels increased nominally linearly with time, indicating that injection did not affect flow rate into the tank for all of the examined dye delivery rates: the system was capable of delivering dye to the model at different concentrations without affecting flow conditions. The setup was therefore incorporated into the centrifuge apparatus according to the hydraulic diagram shown in Figure 4.

2.2 Centrifuge modelling

Injection testing was carried out in the 1.8m radius beam centrifuge based at the National Geotechnical Centrifuge Facility at the University of Western

Figure 4: Centrifuge water supply hydraulic diagram incorporating dye injection system

Table 1: Model layer properties. e_0 void ratio under no effective stress; C_v coefficient of consolidation

Model	Layer	Fine sand (%)	Silt (%)	Kaolin (%)	k_{sat} (μm/s)	e_0	C_v (m2/year)
1	Embankment	0	100	0	3.71–4.55	1.59	2.88×10^3–1.08×10^5
2	Embankment	0	100	0	3.71–4.55	1.59	2.88×10^3–1.08×10^5
	Base	10	90	0	0.31[a]	0.60	11.85
3	Embankment	31	43	26	3.14×10^{-3}–4.25×10^{-2}	1.06	12.53–118.04

[a] constant over stress range of interest;

is discussed in detail in Beckett et al. (2016).

The full study comprised 18 steady-state and drawdown seepage tests, completed over three rounds on models of increasing geotechnical complexity: *1)* (nominally) uniform material; *2)* two (nominally) uniform strata of differing permeabilities; *3)* heterogeneous material. Flow tracing methods were examined in the concluding test of each round, to attempt to visualise the phreatic surface. Soil properties for each of the models are given in Tables 1 and 2. Materials were selected to be increasingly representative of real tailings; provided that the model Reynolds number is sufficiently low, using the same material in the model as in the prototype ensures similar seepage conditions between the two (Hensley and Schofield 1991). Models were manufactured from a slurry (45% water content) of the given materials (representative of field deposition), poured into the model compartment within the strongbox. Material was then centrifugally consolidated and dewatered at an acceleration of $100g$, removed from the centrifuge and cut to the desired profile, shown in Figure 5 (at prototype scale); methods used to convert lengths and head levels to prototype scale are described in Beckett et al. (2016). Sand filters of average hydraulic conductivity (k_{sat}) 3.49mm/s and void ratio (e) 0.62 abutted the models (within the model compartment) to protect the upstream and downstream reservoir membranes. Reservoirs were filled with gravel to provide support to the membranes without hindering flow.

It is noted that traditional tailings deposition methods impart a highly stratified profile whose hydraulic properties can vary by orders of magnitude (Bussière 2007). Layering could not be recreated in the model, however, as scaled layers of representative thickness could not be constructed (can be <1mm at model scale). The models therefore represented bulk TSF seepage behaviour.

Each test assessed the suitability of one tracing fluid: *1)* concentrated acrylic-resin ink (AR); *2)* concentrated food-grade dye (FD); and *3)* sodium fluorescein (FL). All fluids were non-toxic as fluid had to be discharged to the centrifuge chamber during testing. AR and FD are regularly used as flow tracers in flume testing. Fluorescent tracers are commonly used in medical applications as an alternative to coloured dyes; FL is one such tracer, used as it is non-toxic and water soluble. FL angiography can image structures of the order of 1μm, which is typical of tailings pore sizes (Lee et al. 2014). Fluorescein concentra-

Table 2: Individual material component properties. $d_1 0$, $d_5 0$ & $d_6 0$: 10, 50 and 60% mass passing particle diameters; PL: Plastic limit; LL: Liquid limit

Material	$d_1 0$ (μm)	$d_5 0$ (μm)	$d_6 0$ (μm)
Filter sand	300	497	529
Fine sand	124	195	211
Silt	3.2	19.7	27.1
Material	PL (%)	LL (%)	
Kaolin	27[a]	61[a]	

[a] (Cocjin et al. 2014);

tions of up to 100ppm in water (0.1g/L) cause negligible changes to density, viscosity or surface tension (Timmons et al. 1971, Palladini et al. 2005): 100ppm FL was used in this study. Dry fluorescein is an orange powder but forms a yellow-green liquid when mixed with water. It fluoresces green under UV light, which provides a good distinction between it and a nominally-red background, e.g. geotechnical materials. Fluorescein detection can be enhanced by filtering the absorbed (495nm) and emitted (525nm) wavelengths (Keith 1968). Filters were obtained from the UWA Lions Eye Institute and mounted to a UV light source (installed above the camera) and camera respectively.

Tracer fluid injection commenced from a condition of steady-state seepage at $100g$; processes used to establish this seepage regime are described in detail in Beckett et al. (2016). Upstream and downstream water levels at the point of injection are shown in Figure 5 (at prototype scale). Fluid was injected into the centrifuge water supply, which fed into the top of the upstream reservoir. In Models 1 and 2, a single syringe barrel was injected to observe pulse migration. In Model 3, multiple (consecutive) barrels, filled via an additional reservoir (shown in Figure 4), were used to flush the model with FL solution to observe the entire phreatic surface. Fluids were injected at a pressure equal to that of the supply to limit dilution on entering the stream; under such conditions, the water supply was effectively cut off and replaced with the dye stream for the duration of injection.

3   RESULTS AND DISCUSSION

Changes in head level during injection are shown in Figures 6a, c and e for Models 1, 2 and 3 respectively, alongside example images showing the fluid's progress. Note that test times are at model scale; tim-
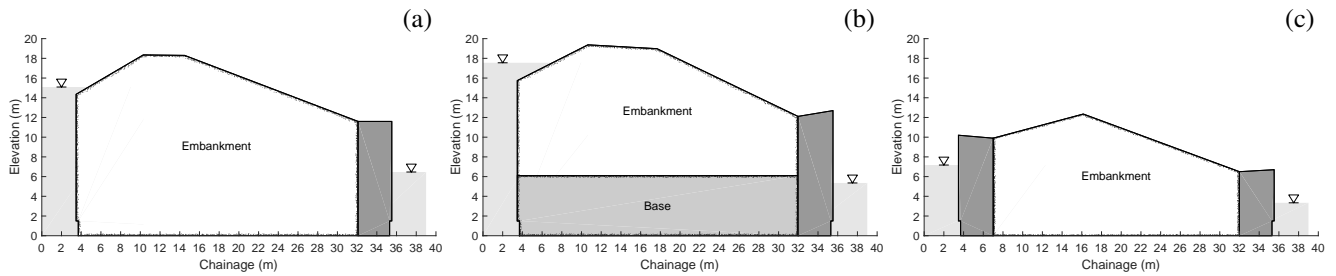
Figure 5: a-c: Model 1-3 profiles at prototype scale. Chainage originates at the upstream reservoir. Light grey zones show upstream (leftmost) and downstream (rightmost) water levels. Dark grey zones show sand filters

ing began at the point of injection into the water supply, i.e. some time elapsed before fluids appeared in the model.

3.1 Model 1: Acrylic-resin ink

AR was visible in the upstream and downstream reservoirs roughly 1000s and 3000s after injection respectively. The downstream reservoir was clear after roughly 5000s. Head levels were nominally constant at all points throughout the test: AR was successfully injected without affecting steady-state seepage conditions. However, regular head 'beats' were detected on all PPTs (Figure 6a). These occurred as flow was collected in the downstream reservoir whilst purging the downstream pump, the effect of which was communicated back up the hydraulic gradient. Consequently, these beats diminished with distance from the downstream reservoir. Figure 6a shows that head levels on all PPTs rapidly returned to steady-state conditions after purging was complete.

AR was visible (faintly) in the downstream sand filter, indicated in Figure 6b, indicating that it might be suitable for examining flow phenomena in granular materials. Unfortunately, it was not detected in the main body of the model, either visually or by analysing changes in pixel colour intensities (using a similar method to that described in Beckett et al. (2016)). AR was therefore not suitable for tracing the phreatic surface or the migration of a single pulse for this model.

3.2 Model 2: Food-grade dye

PPT responses during FD injection are shown in Figure 6c; the injected pulse partway through testing is shown in Figure 6d. Given the higher viscosity, FD pulse migration took significantly longer than AR: roughly 7 hours at model scale. Such times might be prohibitive given the high cost of centrifuge testing.

Unlike AR, FD was visible in the model material. Colouration was the most intense around the lower, less permeable base stratum, due to lower seepage velocities. Figure 6d also shows dispersed dye close to the embankment crest due to capillary uptake and flow above the phreatic surface (flow in the saturated and unsaturated regions was discussed in (Beckett and Fourie 2016)).

Notably, introducing FD into the water feed reduced the delivered flow velocity, causing a drop in head throughout the model (most strongly at the upstream reservoir). Upstream head level dropped dramatically on the pulse entering the reservoir, at 1500s, the effect of which propagated down the hydraulic gradient. Upstream head levels recovered to steady-state values as the pulse passed into the model. The pulse's transition is seen as subsequent 'rebounding' of head levels at roughly 8000, 1200, 15000 and 18000s in Figure 6c for PPTs 1, 2, 3 and 4. It should be noted, however, that changes in head level during rebound events was less than 2% that occuring due to pump purging in Model 1 for AR. Head level changes were due to the FD's high (with respect to water) viscosity, which reduced local flowrate, and so head, when upstream of a given transducer. Times between rebound events and rebound amplitudes reduced as the pulse progressed: dispersion (reducing the pulse's local viscosity) and the model's tapering shape increased local flowrate (approaching that of water) towards the downstream reservoir. Clearly, diffusion and viscosity effects therefore preclude FD from tracing steady-state groundwater phreatic surfaces. However, capturing unequal seepage velocities may be useful when examining migration of a dense contaminant, for example DNAPLs.

3.3 Model 3: Fluorescein

Head level changes during FL injection are shown in Figure 6e. Multiple consecutive syringe barrels were injected (facilitated by an additional dye reservoir, Figure 4) to capture the entire phreatic surface. Excepting in the downstream reservoir, PPT responses showed little fluctuation during injection, indicating steady-state conditions throughout the test. Small downstream head fluctuations (roughly ±0.1mm at model scale) were due to a feedback error on the syringe control loop which generated excessive signal noise.

Available camera exposure times ($\leq$5s) were insufficient to capture fluorescence when the adsorption filter was fitted; the filter was therefore removed, increasing model illumination but creating an additional glow above the model due to the visible light component of the UV light source. The glow notwithstanding, FL provided an excellent contrast between

the wet and dry portions of the sand filters, seen to the left and right hand sides of Figure 6f, using a 4s exposure time. FL also highlighted a large transverse crack within the embankment; the crack formed during steady-state testing but was thought closed. Rather, FL demonstrated that it was filled with coarser debris, forming a preferential seepage path (compromising the model). The phreatic surface in the main body, however, could not be identified: what fluorescence there was was masked by other sources. Re-incorporating the light filter may alleviate this issue, however exposure times greater than those permitted using the current software (limited to 5s) must be accommodated. FL's low viscosity and ready detection may, however, provide an excellent tool to visually verify steady-state phreatic surfaces and model integrity.

4 CONCLUSIONS

This paper presented a method to visually trace seepage flows through a geotechnical centrifuge model. Three models of increasing geotechnical complexity were tested under stress levels representative of full-scale tailings dams. Hydraulic gradients were imposed by controlling water levels upstream and downstream of the models and internal head levels monitored via base-mounted pressure transducers. Tracing dyes were injected on reaching steady-state conditions. Three fluids were investigated: acrylic-resin ink; food-grade dye; and fluorescein. The first two fluids were readily available and all three are non-toxic. Fluorescein is regularly used in medical applications to examine the structures of micron-sized features.

Benchtop testing at $1g$ demonstrated the developed apparatus' ability to deliver a tracing fluid without affecting flow rates into the model. It was therefore incorporated into the main centrifuge apparatus.

Acrylic-resin ink was visible in the highly-permeable sand filters but was unable to create sufficient colour contrast between saturated and unsaturated regions in the main model body. Contrariwise, food-grade dye provided a good contrast throughout the model but its higher viscosity detrimentally affected local flow velocities and head levels: it was not suitable to trace the phreatic surface but might prove a useful tool if examining dense contaminant migration, for example DNAPLs.

Fluorescein provided excellent distinction between saturated and unsaturated regions of high permeability without affecting steady-state head levels. A previously undetected longitudinal crack within the model was also highlighted. Any fluorescence from the main body was, however, masked by brighter regions; incorporating camera and light filters and increasing image exposure times would alleviate this issue. This study therefore demonstrated the potential for fluorescein injection to identify seepage surfaces or pathways in centrifuge models.

REFERENCES

Beckett, C. T. S. & A. B. Fourie (2016, 15–17 March). Centrifuge modelling of drawdown seepage in tailings storage facilities. In A. B. Fourie and M. Tibbett (Eds.), *Mine Closure 2016*, International Conference on Mine Closure, Perth, WA., pp. 271–284. Australian Centre for Geomechanics.

Beckett, C. T. S., A. B. Fourie, & C. D. O'Loughlin (2016). Centrifuge modelling of seepage through tailings embankments. *International Journal of Physical Modelling in Geotechnics 16*(1), 18–30.

Blight, G. E. & A. B. Fourie (2005). Catastrophe revisited — disastrous flow failures of mine and municipal solid waste. *Geotechnical and Geological Engineering 23*, 219–248.

Bussière, B. (2007). Colloquium 2004: Hydrogeotechnical properties of hard rock tailings from metal mines and emerging geoenvironmental disposal approaches. *Canadian Geotechnical Journal 44*(9), 1019–1052.

Cocjin, M., S. Gourvenec, D. White, & M. Randolph (2014). Tolerably mobile subsea foundations — observations of performance. *Géotechnique 64*(11), 895–909.

Hensley, P. J. & A. N. Schofield (1991). Accelerated physical modelling of hazardous-waste transport. *41(3)*(3), 447–465.

Keith, C. G. (1968). Fluorescence ophthalmoscopy. *British Journal of Ophthalmology 52*, 862–863.

Lee, J. K., J. Q. Shang, & S. Jeong (2014). Thermo-mechanical properties and microfabric of fly ash-stabilized gold tailings. *Journal of Hazardous Materials 276*, 323–331.

Palladini, L. A., C. G. Raetano, & E. D. Velini (2005). Choice of tracers for the evaluation of spray deposits. *Sci. Agric. (Piracicaba, Braz.) 62*(5), 440–445.

Stanier, S., J. Blaber, W. Take, & D. White (2015). Improved image-based deformation measurement for geotechnical applications. *53*, 727–739.

Timmons, D. R., C. K. Mutchler, & E. M. Sherstad (1971). Use of fluorescein to measure the composition of waterdrop splash. *Water Resources Research 7*(4).
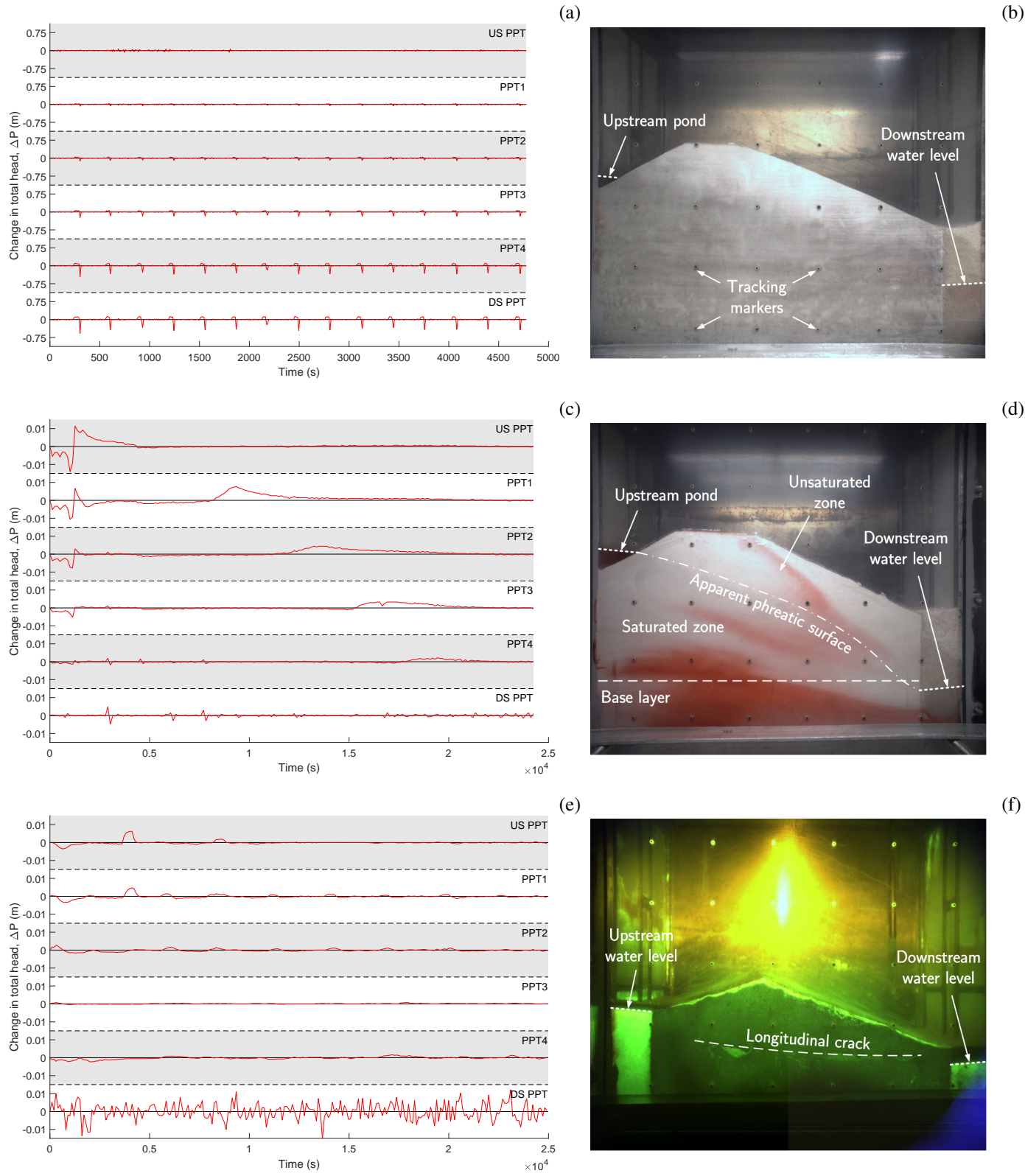
Figure 6: Change in total head (prototype scale), recorded at base-mounted pore pressure transducers (PPTs) during injection (left) and example image of injected fluid (right). Times are at model scale. Top: Model 1 (AR); middle: Model 2 (FD); bottom: Model 3 (FL). "US": upstream; "DS", downstream